Geomechanics and Engineering, *Vol. 31, No. 1 (2022) 53-69*
https://doi.org/10.12989/gae.2022.31.1.053

Numerical investigation of responses of a piled raft to twin excavations: Role of sand density

Hemu Karira[1], Aneel Kumar[2], Tauha Hussain Ali[2], Dildar Ali Mangnejo*[1] and Li Yaun[3]

[1]*Department of Civil Engineering, Mehran University of Engineering and Technology, Shaheed Zulfiqar Ali Bhutto Campus, Khairpur Mir's, Sindh, Pakistan*
[2]*Department of Civil Engineering, Mehran University of Engineering and Technology, Jamshoro, Sindh, Pakistan*
[3]*School of Mechanics and Civil Engineering, China University of Mining and Technology, Xuzhou, Jiangsu, P.R. China*

(*Received July 18, 2022, Revised August 21, 2022, Accepted September 14, 2022*)

Abstract. In densely built areas, the development of underground transportation systems often involves twin excavations, which are sometimes unavoidably constructed adjacent to existing piled foundations. Because soil stiffness degrades with induced stress release and shear strain during excavation, it is vital to investigate the piled raft responses to subsequent excavation after the first tunnel in a twin-excavation system. The effects of deep excavations on existing piled foundations have been extensively investigated, but the influence of twin excavations on a piled raft is seldom reported in the literature. In this study, three-dimensional numerical analyses were carried out to investigate the influence of sand density on an existing piled raft (with a working load on top of the raft) due to twin excavations. A wide range of relative density (D_r) from loosest (30%), loose to medium (50% and 70%), and densest (90%) were selected to investigate the effects on settlement and load transfer mechanism of the piled raft during twin excavations. An advanced hypoplastic sand model (which can capture small-strain stiffness and stress-state dependent dilatancy of sand) was adopted. The model parameters are calibrated against centrifuge test results in sand reported in the literature. From the computed results, it is found that twin excavations in loose sand (D_r=30%) caused the most significant settlement. This is because of the higher stiffness of denser sand (D_r=90%) than that of loose sand. In contrast, a much larger tilting (maximum magnitude=0.18%) was computed in dense sand than in loose sand after the completion of the first excavation. As far as the load transfer mechanism along the piles is concerned, an upward load transfer to mobilize shaft resistance is observed in loose sand. On the contrary, a downward load transfer is observed in dense sand.

Keywords: load transfer; piled raft; sand density; tilting; twin excavations

1. Introduction

It is well-known fact that a pile supports a load of the superstructure by transferring it to the ground resulting in the generation of stresses surrounding the piled foundation (Fang *et al*. 2022). On the contrary, excavation is a stress relief process that results in ground movements (which appear on the ground surface as a settlement trough behind the diaphragm wall) around the excavation (Soomro *et al*. 2021c). The expansion of cities and urban areas is resulting in an increased demand for environmentally and economically sustainable transport and services infrastructure (e.g., water, waste, etc). Underground construction and infrastructure often require underground construction. For public convenience, basement excavations for shopping malls and (or) car parks are often constructed adjacent to the existing piled supported structures (Shi *et al*. 2022a, Finno *et al*. 1991, Korff 2016, Soomro *et al*. 2021a). Hence, excavation remains a big challenge for geotechnical engineers, particularly when an excavation is to be carried out adjacent to the buildings resting on piled foundations. Therefore, it is vital predicting the responses of pile foundation to an adjacent excavation so that measures can be taken to minimize the impact of the ground deformation on the building. To assess basement excavation-induced potential adverse effects on existing pile foundations, many studies have been conducted to explore excavation-induced bending moment and lateral deflection in exiting piles via field tests (i.e., Finno *et al*. 1991, Goh *et al*. 2003), centrifuge tests (i.e., Leung *et al*. 2000, 2003, Ng *et al*. 2017) and numerical modelling (i.e., Poulos and Chen 1996, 1997, Liyanapathirana and Nishanthan 2016, Lee 2019, Qian *et al*. 2020). In those studies, negligible pile settlements were induced by basement excavation. Thus, all these research findings may be applicable for end-bearing piles. By conducting theoretical analyses, deep excavation-induced pile settlements were significantly affected by the working load, soil movements, and end bearing capacity (Korff *et al*. 2016). Based on centrifuge and numerical modelling, several studies found that basement excavation-induced additional settlements of floating piles could not be ignored (Ng *et al*. 2017, Shi *et al*. 2019). Most previous studies have focused on the effects of a single excavation on single piles and pile groups. In fact, twin excavations are particularly favoured across the world when developing underground transportation systems (Chen *et al*. 2013, Zeng *et al*. 2018). Shi *et al*. (2022b) performed centrifuge tests and conducted numerical modelling to investigate the

*Corresponding author, Ph.D. Student
E-mail: dildarali@muetkhp.edu.pk

ISSN: 2005-307X (Print), 2092-6219 (Online)

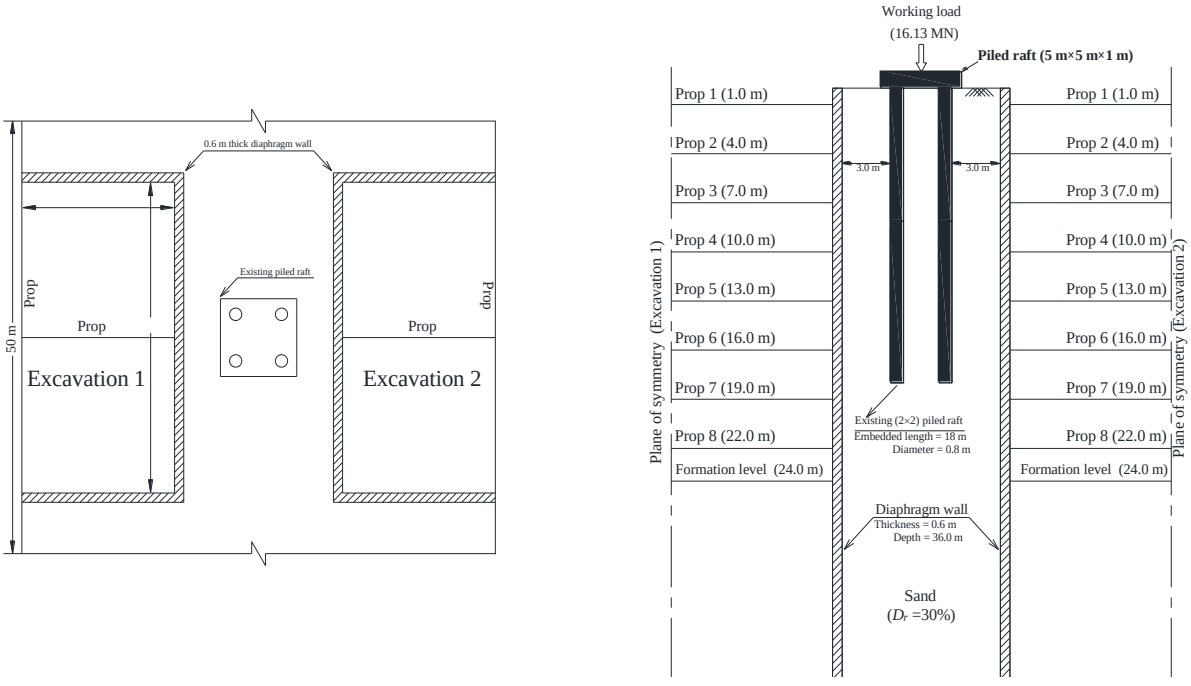

(a) (b)

Fig. 1 Configuration of numerical simulation (a) plan view (b) Elevation view

effects of double basement excavations on an existing floating pile in dry sand. They concluded that upon completion of double excavations simultaneously, the maximum pile bending moment is only 0.34 *Mc* (pile bending moment capacity), which is only 18.9% of that due to double excavations excavated sequentially. Previous studies related to excavation-structure interaction mainly focused on the performance of a single excavation. In contrast, only limited studies have investigated the effects of double excavation on the deformation behaviour of adjacent foundations. However, most of the previous studies have focused on the effects of excavation effects on single piles and pile groups. Much less attention has been paid to the effects of twin excavations on the piled raft, which are normally used to support high-rise buildings (Roy *et al*. 2020, Bhaduri and Choudhury 2020). It is likely that twin excavations adjacent to an existing pile group would result in complicated load transfer within each pile in the piled raft, as well as load redistribution among the piles.

To investigate the settlement, tilting, load transfer, and load redistribution of a piled raft affected by twin excavations in sand with different densities (i.e., D_r=30%, 50%, 70%, and 90%), three-dimensional numerical analyses were conducted. Soil responses were simulated by a hypoplastic (sand) model with an intergranular strain concept which has the ability to capture the small-strain soil stiffness and stress-state dependent dilatancy.

2. Three-dimensional finite element analysis

2.1 Characteristics of the numerical model

Three-dimensional Since the soil behaviour is highly dependent on soil density, the effects of sand relative density (D_r) on piled raft responses to twin excavations were investigated in this study. A wide range of relative density (D_r) from loosest (30%), loose to medium (50% and 70%), and densest (90%) were selected to investigate the effects on settlement and load transfer mechanism of the piled raft during twin excavations. To enhance the fundamental understanding of stress transfer and soil stiffness around the existing piled raft, three-dimensional numerical analyses were carried out using the software package Abaqus (Hibbitt *et al*. 2010). In this study, a (2×2) piled raft with embedded length (L_p)=18 m and pile diameter (d_p)=0.8 m is considered.

The piled raft is subjected to a working load of 16.13 MN. Twin excavations (one after the other) were carried out adjacent to the existing piled raft (see Fig. 1(a)). Fig. 1(b) shows the elevation view of the configuration of numerical simulation in which twin excavations were carried out adjacent to the piled raft in sand with D_r=30%. Twin excavations (each of a final excavation depth (H_e) of 24.0 m and a width of 10.0 m) were simulated in the numerical analysis, while the length of each excavation was taken as 20 m. For both excavations, the diaphragm walls had a depth of 36 m with an embedded depth of the wall in the ground (i.e., penetration depth (H_p)) of 12 m (see Fig. 1(b)). Therefore, the value of the wall penetration ratio (H_p/H_e) becomes 0.5, which is a typical penetration depth ratio in engineering practice (Ng *et al*. 2021, Shi *et al*. 2019, Karira *et al*. 2021, Soomro *et al*. 2021b). The clear distance between diaphragm wall and the pile is 3.0 m. The props are provided to support the lateral movement of the diaphragm wall due to the earth pressure behind the wall. By installing more props, horizontal movements of the wall and soil can be reduced. The behaviour of props is generally

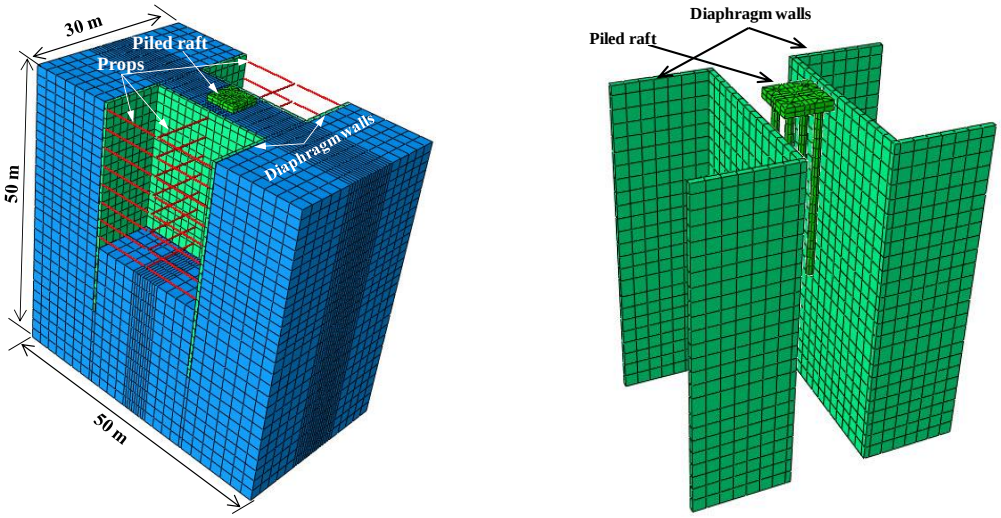

(a) (b)

Fig. 2 (a) 3D numerical model mesh (b) the mesh of the piled raft and diaphragm walls

evaluated based on the axial compressive loads (Soomro *et al*. 202c, Hong *et al*. 2017). Eight levels of props supported the diaphragm walls in both excavations with a vertical and horizontal spacing of 3.0 m and 5 m, respectively. The first level of props was installed at 2.0 m below the ground surface. The props (I-section) are modelled as soft with axial rigidity of 81×10^3 kNm (Shi *et al*. 2019).

2.2 Finite element mesh and boundary conditions

Fig. 2(a) shows an isometric view of a typical finite element mesh. The depth from the ground surface to the base of the mesh was 50 m. Eight-noded hexahedral brick elements were used to model the soil, piled raft, and the diaphragm wall, while two-noded truss elements are adopted to model the props. In the analysis, the piled raft installation effect on in situ stress distribution of soil was not considered, and hence the "wished-in-place pile" was modelled. Therefore, the behaviour of the pile may be quite close to a bored pile. The obtained computed results can be conservative with this assumption. Roller and pin supports are applied to the vertical sides and the base of the mesh, respectively. Therefore, movements normal to the vertical boundaries and in all directions of the base are restrained. The pile-soil and wall-soil interface is modelled as zero thickness by using duplicate nodes. The interface is modelled by the Coulomb friction law, in which the interface friction coefficient (μ) and limiting displacement (γ_{lim}) are required as input parameters. A limiting shear displacement of 5 mm is assumed to achieve full mobilization of the interface friction equal to $\mu\times$p', where p' is the normal effective stress between two contact surfaces, and a typical value of μ for a bored pile of 0.35 is used in all analyses (Soomro *et al*. 2021d, Soomro *et al*. 2022b).

2.3 Constitutive model and model parameters used in finite element analyse

An advanced hypoplastic model was used to simulate the behaviour of sand in this study. The hypoplastic model was developed to describe the non-linear response of granular material (Gudehus 1996, Herle and Mašín 1999). It consists of eight model parameters (ϕ'_c, h_s, n, e_{d0}, e_{c0}, e_{i0}, α and β). The first six parameters (ϕ'_c, h_s, n, e_{d0}, e_{c0}, e_{i0}) of Toyoura sand were calibrated by Herle and Gudehus (1999). The remaining two parameters (α and β) were obtained by curve fitting Maeda and Miura (1999)'s triaxial test results (at large strains). To account for strain-dependency and path-dependency of soil stiffness (at small strains), Niemunis and Herle (1997) further improved the hypoplastic model by incorporating the intergranular strain concept into the model. Five additional parameters (m_R, m_T, R, β_r, and χ) are required. These five parameters were obtained by fitting the stiffness degradation curves of Toyoura sand obtained from the stress-path triaxial tests carried out by Hong *et al*. (2017). The model parameters were taken from a study by Shi *et al*. (2019). They calibrated and validated all the parameters of the hypoplastic sand model against their centrifuge test results (which was performed to simulate excavation in sand). The coefficient of at-rest earth pressure (K_0=0.5) was estimated based on the effective angle of shearing resistance at the critical state (ϕ'=31°, as reported by Ishihara 1993) and Jáky (1944)'s equation. Table 1 summarises the model parameters of Toyoura sand adopted in the numerical analyses. The concrete pile, the diaphragm wall, and the props were assumed to be linear elastic with Young's modulus of 35 GPa and Poisson's ratio of 0.25. The unit weight of concrete was assumed to be 24 kN/m^3.

2.4 Numerical simulation

Over the previous decades, many researchers have used different numerical methods to simulate excavation in the ground (Hong *et al*. 2017). In this study, finite element modelling using Abaqus software was used to simulate the three-dimensional interaction of twin excavations and piled raft foundations in sandy soil. The numerical simulation in

Table 1 Hypoplastic model parameters of sand adopted in this study

Description	Parameter
Effective angle of shearing resistance at critical state: ϕ_c	31°
Hardness of granulates, h_s	2.6 GPa
Exponent n	0.27
Minimum void ratio at zero pressure, e_{d0}	0.61
Maximum void ratio at zero pressure, e_{c0}	1.10
Critical void ratio at zero pressure, e_{i0}	0.98
Exponent α	0.14
Exponent β	6
Parameter controlling initial shear modulus upon 180° strain path reversal, m_R	11
Parameter controlling initial shear modulus upon 90° strain path reversal, m_T	6
Size of elastic range, R	2×10^{-5}
Parameter controlling degradation rate of stiffness with strain β_r	0.1
Parameter controlling degradation rate of stiffness with strain χ	1.0

this study was carried out in the following steps:

(i) The initial stresses of the soil were established by applying a gravity load and the coefficient of lateral earth pressure using the Jáky (1944)'s equation.

(ii) The piled raft foundation on top of the soil deposit and then subjected to a working load of 16.13 MN.

(iii) Construct the diaphragm wall for the first excavation.

(iv) Excavate the first stage of the first excavation by deactivating the soil elements. After excavating to 3 m depth, the first level of props is installed at 1 m below the ground surface.

(v) Similarly, the next stages were excavated and props installed until the last stage of excavation (i.e., H_e=24 m) is completed.

(vi) Repeating the same procedure as in (*iv*) and (*v*), the second excavation was carried out.

3. Interpretation of computed results

3.1 Effects twin-excavation induced settlement of the piled raft

Fig. 3 shows the normalised incremental settlement of the piled raft (S_p/d_p) constructed in the sand with different values of relative densities of D_r=30%, 50%, 70%, and 90% during twin excavations. The excavation stages of each excavation depth are represented by h. The piled raft settlement and excavation depths (h) are normalised by pile diameter (d_p) and final excavation depth (H_e=24 m), respectively. For comparison, measured settlement of a single pile (diameter of pile=0.8 m with embedded length=20 m in prototype) due to double excavation (first multi-propped and second cantilever excavation) in the dry sand of D_r=70% measured in centrifuge test (by Shi *et al.* 2022b) is also included.

It can be observed that the rate of S_p increased with the first excavation stages in the sand with different relative densities. This is because of the degradation of stiffness of sand due to excavation-induced stress release and shear strain surrounding the pile. With increasing depth of excavation in the sand with different relative densities, the stiffness of the sand degraded resulting in larger settlement during subsequent excavation stages (discussed in section 3.3). During each stage of the first excavation, the induced settlement of the piled raft in denser sand is smaller as

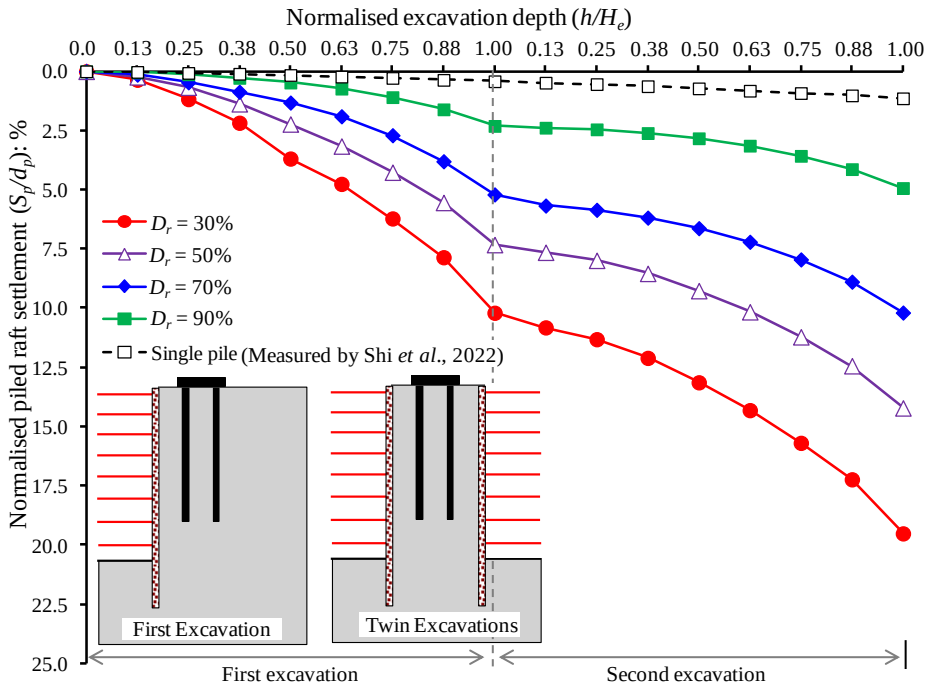

Fig. 3 Induced settlment of the pile raft during twin excavations

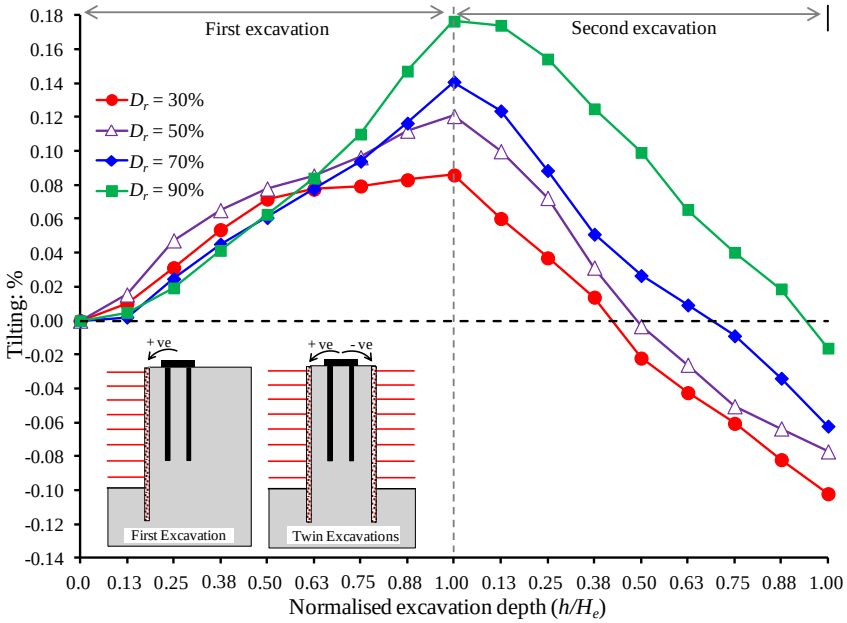

Fig. 4 Induced tilting of the raft during twin excavations

compared in sand loose sand. This observation can be attributed to the higher stiffness of denser sand than that of loose sand. As shown in the figure similar characteristics of the first multi-propped excavation-induced settlement of a single pile were observed from the centrifuge test reported by Shi *et al.* (2022b). However, the final measured induced settlement of a single pile is smaller than that of the piled raft. This can be attributed to the working load and excavation depth. The working load applied on the single pile is smaller than that on the piled raft and the final depth of adjacent excavation is only 9 m. The induced final piled raft settlements after the completion of the first excavation in the sand of relative densities of D_r=30%, 50%, 70%, and 90% were 82, 59, 42, and 19 mm (i.e., 10.2, 7.3%, 5.2% and 2.3% of the pile diameter), respectively. During the second excavation, the characteristics and magnitudes of piled raft settlement are similar to those observed during the first excavation in the sand with different relative densities. The induced settlement due to second excavation is also decreased with the increasing density of sand. This is because of the raft (resting on the ground) attached to the four piles. The load resisted by the raft decreased during the first three stages of the first excavation but increased till the completion of the excavation. This resulted in penetration of the raft in the ground led to an increment of sand stiffness underneath the raft. Hence, the subsequent excavation caused a similar settlement quantitatively. The computed results in this study have revealed that the principle of superposition may be used in predicting the settlement of the piled raft due to the second excavation. Unlike the induced settlement of the piled raft during the second excavation, the second excavation caused a larger single pile settlement than that due to the first excavation (reported by Shi *et al*. 2022b). This is because soil stiffness is reduced after multi-propped excavation and a much softer supporting system of cantilever excavation. The additional amounts of settlement due to the second excavation in sand of relative densities of D_r=30%, 50%, 70% and 90% were 80, 55, 40 and 20 mm (i.e., 10.0%, 6.9%, 5.0% and 2.5% of the pile diameter), respectively.

3.2 Induced tilting during twin excavations

It is well-recognized that excavation essentially induces stress relief in the ground which resulted in a ground movement towards the excavation. On the other hand, high-rise buildings are normally founded on the piled raft to avoid differential settlement in the building (Bhaduri and Choudhury 2021, Poulos 2001). When an excavation is carried out adjacent to piled raft, differential settlement can likely be induced in the raft. Hence, it is necessary to understand the tilting mechanism of the piled raft during twin excavations. The differential settlement is presented in terms of tilting which is defined as the ratio of the differences in the settlement between the two edges of the piled raft and the distance between the edges. Tilting toward the first excavation is taken as positive vice-versa. Fig. 4 compared the induced tilting of the piled raft in the sand of different relative densities (i.e., D_r=30%, 50%, 70%, and 90%) during the first and the second excavations. It can be observed from the figure that the positive tilting increased non-linearly during the first excavation in all four cases. This is because the piled raft is subjected to the non-uniform and only at one side stress release during the first excavation (discussed in section 3.4). The row of piles nearest the excavation (i.e., front row) is subjected to higher stress release than that of farthest the excavation (i.e., rear row). Consequently, the front row piles settled larger than that of the rear row due to excavation which caused differential settlement in the piles. The working load was re-distributed among four piles and the raft due to excavation-induced tilting of the piled raft (discussed in section 3.7). Furthermore, the rate of induced tilting in very loose to loose sand (i.e., D_r=30% and 50%) decreased as the

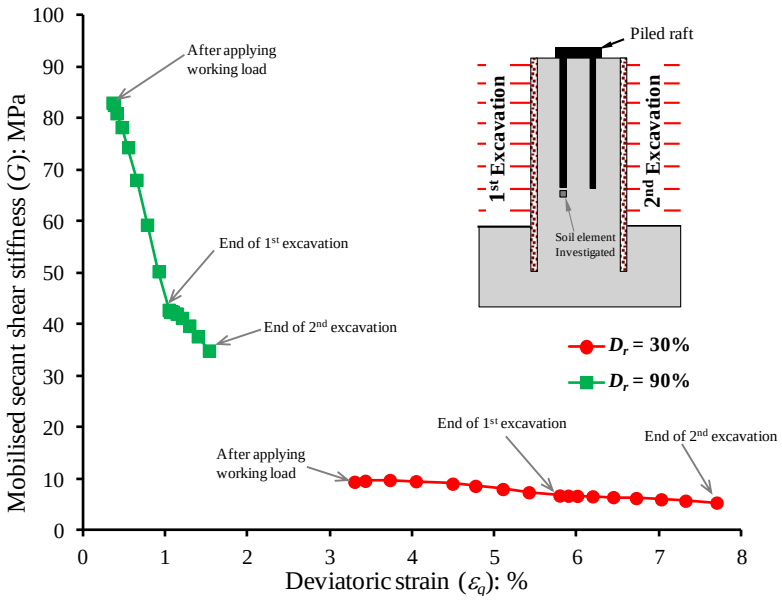

Fig. 5 Mobilised shear stiffness of soil element underneath the pile toe during twin excavtions

excavation depth increases. However, the rate of the positive tilting increased in medium to very dense sand (i.e., D_r=70% and 90%)) as excavation stages further proceeded after h/H_e=0.75. Unlike the induced settlement of the piled raft, the induced tilting of the piled raft in dense sand was larger than that in loose sand. This is because of the ground movement and shear strain induced due to excavation. In loose sand (D_r=30%), the zone of the ground movement and shear strain due to excavation is larger and wider than that of dense sand (discussed in section 3.5). The row of piles closets to the excavation in dense sand is severely affected as compared to that farthest to the excavation. A smaller amount of tilting (0.08%) therefore resulted in the loose sand test than in dense sand (0.17%) on completion of the first excavation.

During the subsequent excavation (which is carried out on the other side of the piled raft, see inset in the figure), the measured tilting decreases non-linearly as the second excavation depth increases in all four cases. As a result, the piled raft tilts towards the second excavation. In contrast to the tilting after the first excavation, the final tilting of the piled raft due to the second excavation in very loose to loose sand (D_r=30% and 50%) is larger than that in dense sand. This excavation-induced settlement mechanism can be attributed to the degradation of clay stiffness around the piled raft due to stress release and the development of shear strains as a result of the second excavation. The stiffness of the soil element underneath piles degraded due to the first excavation-induced stress release before the second excavation (discussed in section 3.3). As a result, the induced tilting of the piled raft caused by the second excavation was greater than that caused by the first excavation. On completion of the second excavation in sand of relative densities of D_r=30%, 50%, 70% and 90% were -0.11%, -0.08%, -0.06% and -0.02%, respectively. To avoid any collapse/damage in the buildings, there are guidelines provided by the design codes. Eurocode 7 (2001) recommends a wide range of the maximum acceptable tilting (1/2000 to 1/300) for different types of structures (i.e., load-bearing or continuous brick walls, open-framed structures, in-filled frames).

3.3 Mobilized shear stiffness due to twin excavations

To fully understand the settlement and the lateral displacement mechanisms induced in piled raft due to twin excavations, mobilized secant shear stiffness and underneath the pile toe along soil column is interpreted in this section. The mobilized secant shear modulus (G_m) values were calculated from the following equations

$$G_m = q/3\varepsilon_s \quad (1)$$

$$q = \frac{1}{\sqrt{2}}\sqrt{[(\sigma_1-\sigma_2)^2+(\sigma_2-\sigma_3)^2+(\sigma_3-\sigma_1)^2]} \quad (2)$$

$$\varepsilon_s = \sqrt{\frac{2}{9}[(\varepsilon_1-\varepsilon_2)^2+(\varepsilon_2-\varepsilon_3)^2+(\varepsilon_3-\varepsilon_1)^2]} \quad (3)$$

where q and ε_s are the computed deviatoric stress and strain, respectively. σ_i and ε_i $(i = 1, 2 \& 3)$ are the principal stresses and strains, respectively.

3.3.1 Mobilised shear stiffness of soil element underneath the pile toe

To fully understand the settlement mechanism of piled raft due to twin excavations mobilized secant shear stiffness of soil element underneath the pile toe in loose (D_r=30%) and dense sand (D_r=90%). Fig. 5 shows the variation of secant shear stiffness (G) of soil element with shear strain (ε_q) underneath the pile toe during the first and second excavations in both cases.

As expected, the degradation of stiffness of the selected element is higher in the case of D_r=30% than in the case of D_r=90%. This is because of the initial stiffness of sand which is higher in case dense sand. The stiffness of the element in the case of D_r=90% decreased due to the first excavation significantly as compared to that in the case of

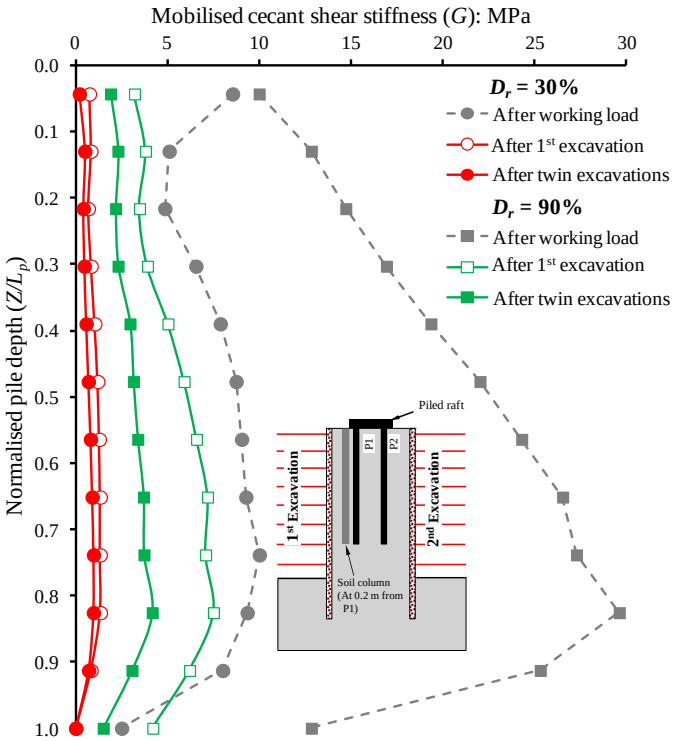

Fig. 6 Mobilised secant shear stiffness of soil elements along the pile after first and second excavations

D_r=30%. This result can be ascribed to an increase in mean effective stress and deviatoric stress resulting from upward load transfer (explained in section 3.11) and a reduction in lateral stresses (explained in section 3.4) in the case of D_r=90%. These changes in stresses led to the failure of the soil element (discussed in section 3.11). Therefore, the stiffness of the soil element decreased substantially. On the other hand, in the case of D_r=30%, negligible changes in stiffness of the element were computed during the first excavation. This is because the load was significant upward load transferred along the piles. The piled raft had to settle to mobilise upward load. As a result, the induced settlement of the piled raft is larger in the case of D_r=30% than that in the case of D_r=90%. Similar to the degradation of stiffness during the first excavation in both cases, the degradation in dense sand is larger than that in loose sand. However, the magnitude of degradation during the second excavation is smaller than that during the first excavation. Hence, the subsequent excavation caused a similar settlement quantitatively (see Fig. 3).

3.3.2 Mobilised shear stiffness along soil column near the piled raft

Fig. 6 shows the secant shear stiffness (G_o) variation along a soil column between the first excavation and the piled raft after completion of the first and twin excavations in the sand with D_r=30% and D_r=90%. After the application of working load on the pile (before excavation), the mobilised soil stiffness decreased along the entire depth of the pile in the case of D_r=30%. Because the higher load is taken by the raft in the case of D_r=30%, the mobilised stiffness at the upper portion of the column is larger than that lower portion. Unlike in the case of D_r=30%, the mobilised stiffness increased along the length of the pile in the case of D_r=90%. This is because the higher initial stiffness and the larger load were transferred to the piles in the case of D_r=90%. Compared to the mobilised stiffness after application in the case of D_r=30%, the stiffness in the case of D_r=90% is higher as expected.

After the first excavation in both cases, the soil stiffness degraded significantly. The stiffness degradation in case of dense sand is smaller than that in case of loose sand (i.e., the maximum degradation 100% in case of D_r=30% and 88% in case of D_r=90%). This is because of stress release near the pile shaft due to the first excavation. Owing to stress release during subsequent excavation, the soil stiffness further degraded along the pile. Similar to the stiffness degradation due to the first excavation, smaller degradation in dense sand was induced after the completion of the second excavation. As discussed in section 3.1, the piled raft settlement due to twin excavations in case of D_r=30% are higher than that in case of D_r=90%. This is due to the reason that degraded soil stiffness along the pile shaft in the case of D_r=30% is larger than that in the case of D_r=90%.

3.4 Changes in horizontal effective stresses due to twin excavations

Figs. 7(a) and (b) show the computed normal stress (horizontal pressure) acting on piled raft prior to and on completion of the first and twin excavations in cases of D_r=30% and D_r=90%, respectively. Two directions were investigated: the front (F) and back (B) of the piled raft (see inset in the figure), which correspond to their location relative to the first excavation. Earth pressure at rest and

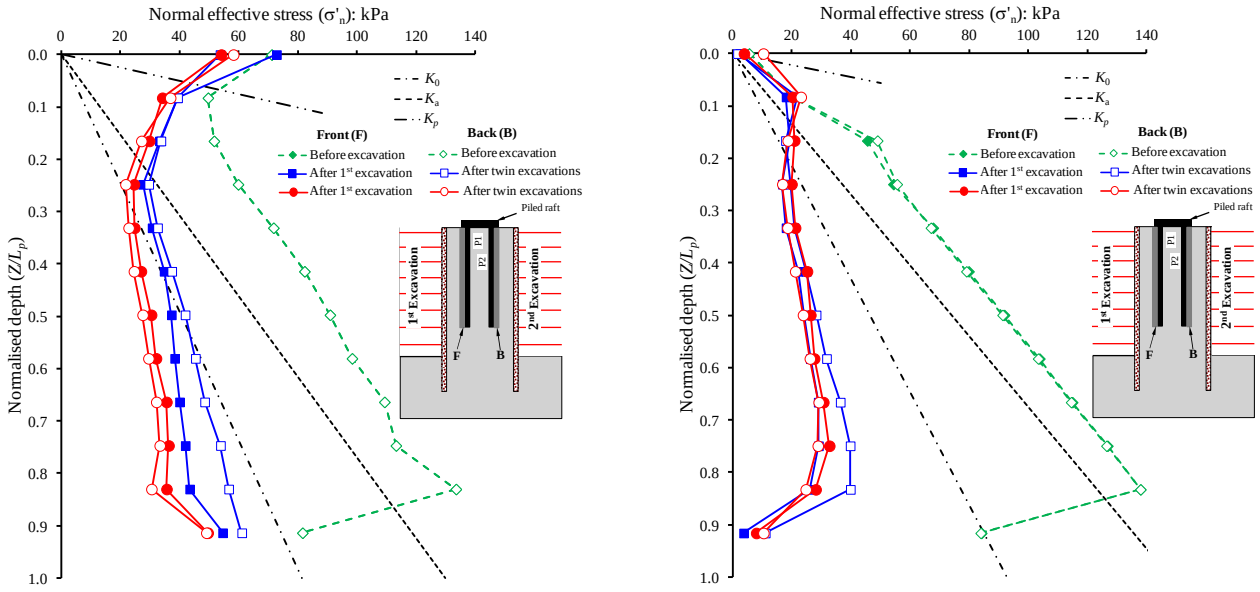

Fig. 7 Computed normal stress acting on the pile (a) D_r=30%, (b) D_r=90%

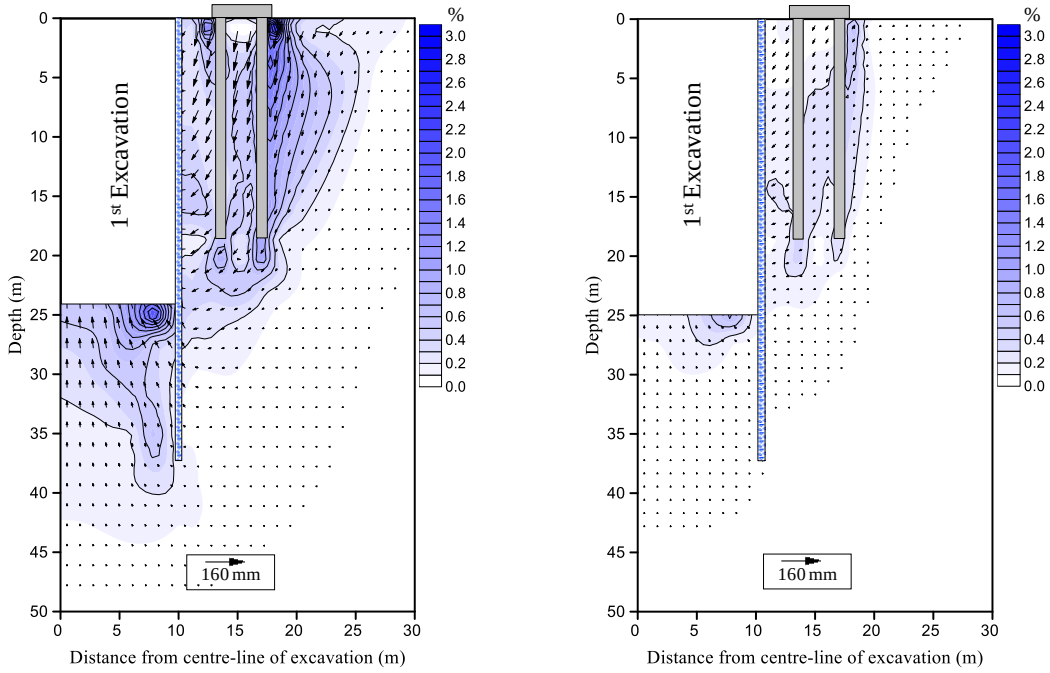

Fig. 8 Computed incremental soil displacement vectors and shear strain after the first excavation (a) D_r=30%, (b) D_r=90%

Rankine active and passive earth pressure (K_o, K_a, and K_p lines, respectively) corresponding to D_r=30% and D_r=90% are included for comparison. Considering the normally consolidated condition, K_o is estimated by $K_0 = (1 - \sin\varphi')$ (Jáky 1944). K_a and K_p are calculated by $K_a = \tan^2(45 - \varphi'/2)$ and $K_p = \tan^2(45 + \varphi'/2)$, respectively. In these equations, φ' is determined as 31°. Thus K_o, K_a, and K_p are 0.51, 0.32, and 3.12, respectively.

Prior to excavation, normal stress acting on the pile in both directions B and F is higher (increasing the passive earth pressure at upper part) than those of earth pressure at rest and Rankine active earth pressure in case of D_r=30%. This is because of the load transferred to the shallower ground by the raft and the mobilization of shaft resistance along the lengths of the piles. In contrast, owing to the smaller load carried by the raft in the case of D_r=90%, the normal stress at the upper part of the pile does not exceed the passive earth pressure (see Fig. 7(b)). It can be observed that after completion of the first excavation, normal stress in both direction F and B decreased dramatically at the lower portion of the pile (i.e., $Z/L_p \geq 0.25$) which are lower than Rankine active earth pressure in both cases. Owing to the reduction in normal stresses in direction F and direction B, the soil would displace towards the first excavation (discussed in section 3.5) and result in differential settlement in the piled raft (see Fig. 3). However, after

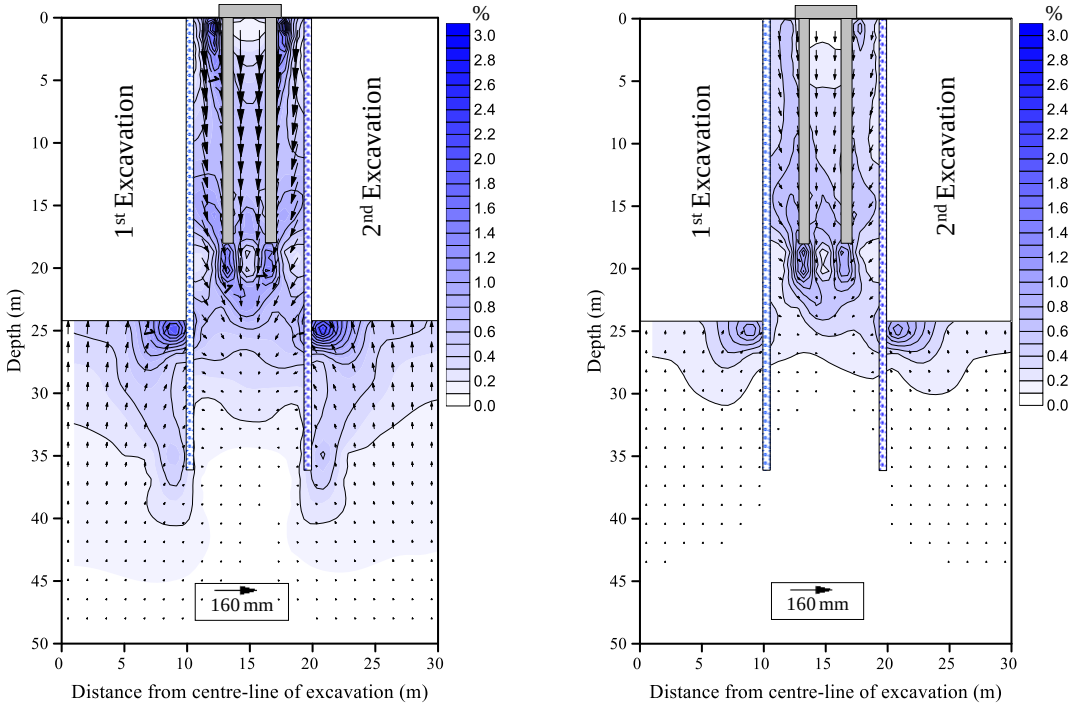

Fig. 9 Computed incremental soil displacement vectors and shear strain after twin excavations (a) D_r=30%, (b) D_r=90%

subsequent excavation on the other side of the piled raft, the in direction F and direction B further decreased causing the piled raft to tilt towards the second excavation (see Fig. 4). Moreover, deflection in the pile and the induced bending moment were reduced. Similar to the case of D_r=30%, the normal stress along the piles decreased in both directions (direction F and direction B) in the case of D_r=90%. Compared to the reduction of the normal stress on the piled raft (with the maximum percentage reduction of 67% at Z/L_p=0.25) in the case of D_r=30%, the reduction of the normal stress (with the maximum percentage reduction of 96% at Z/L_p=0.92) in case of D_r=90% is smaller on completion of the first excavation. This is because of the larger unit weight of sand in case of D_r=90% hence stress release (weight of sand) during excavation is larger than that in case of D_r=30%. Because of load transfer from piles to the raft (discussed in section 3.6), negligible changes in normal stresses on the upper portion of piles were induced.

3.5 Computed ground movement and deviatoric strain due to twin excavations

To understand the influence of sand density on induced settlement and lateral movement of the pile draft, displacement vectors and deviatoric strain contours on the completion of twin excavations were extracted in the soil elements along the monitoring section (see Fig. 1) around the piled raft. Fig. 8(a) and (b) illustrate the displacement vectors on completion of the first excavation in the cases of D_r=30% and D_r=90%, respectively.

In addition, computed incremental shear strain contours induced by twin excavations are also superimposed in the figures. It can be observed that the sand flows towards the first excavation-induced stress release in both cases. Moreover, the lateral movement of the ground occurred near the lower portion of the wall (at 20 m depth of the wall) than at the ground surface. This caused a "bulging" deformation profile of the wall. The soil movement in the loose ground (i.e., D_r=30%) is larger than that in the denser ground (i.e., D_r=90%). As the relative sand density increases from 30% to 90%, the maximum soil movement decreases from 80 mm to 20 mm. This is because of the lower shear modulus of loose sand. The piled raft is located within the major influence zone of ground movement where significant shear strain is developed in the case of D_r=30%. Whereas the toe of pile P1 pile P1 is located within the localised region of induced shear strain. This caused the larger settlement and smaller tilting (differential settlement) of the piled raft in loose sand than that in dense sand. Owing to the smaller lateral movement of the sand due to the first excavation in the case of dense sand compared to loose sand, the induced pile deflection and bending moment in the piles are smaller.

After the completion of twin excavations in cases of D_r=30% (see Fig. 9(a)) and D_r=90% (see Fig. 9(b)), excavation-induced net soil displacement vectors are directed downward. Furthermore, shear strain zones generated due to twin excavations are overlapping each other resulting in an intensive shear strain zone around the piled raft. Similar to the induced ground moment and shear strain due to the first excavation, smaller ground movement and shear strain in dense sand were induced after the completion of the second excavation. As a result, a similar amount of incremental settlement (Fig. 3) and tilting (Fig. 4) of the piled raft is induced by the second excavation, compared to that caused by the first excavation.

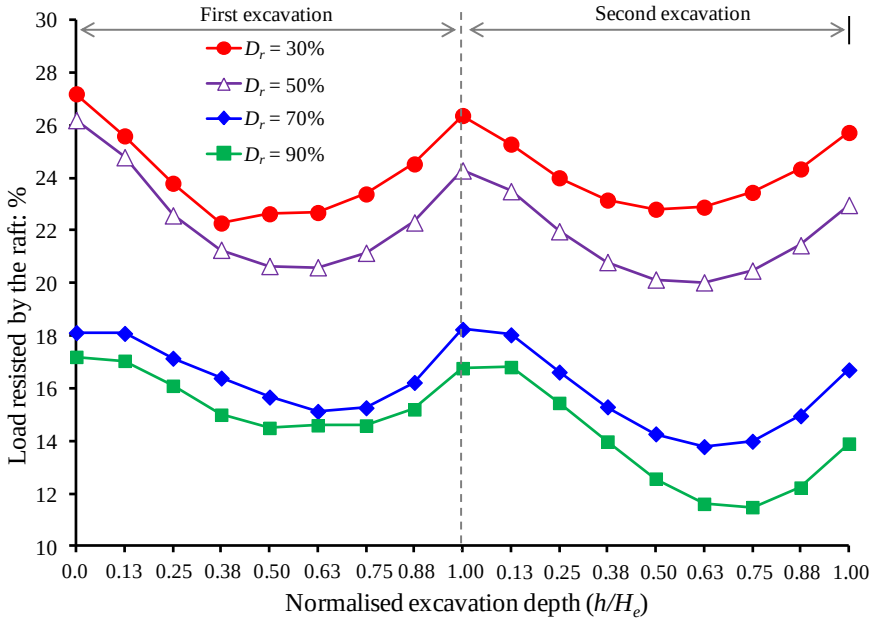

Fig. 10 Changes in load resisted by the raft during twin excavations

3.6 Changes in piled raft load transfer mechanism due to excavation

In a piled raft system, the applied working load is taken by both the piles and the raft prior to excavation. The load redistribution between the raft and piles was observed during twin excavations. Fig. 10 shows the changes in load taken by the raft during the first and second excavations in loose sand (D_r=30%), loose to medium dense sand (D_r=50% and 70%), and dense sand (D_r=90%). It can be observed that the load is taken by the raft in loose sand (27% of the working load in case of D_r=30%) is higher than that in dense sand (17% of the working load in case of D_r=90%) after application of the working load (i.e., 16.13 MN).

This is because the stiffness of loose sand is lower than that of the dense sand which resulted in larger piled raft settlement in case of loose sand due to the application of the working load. Consequently, a larger load was taken by the raft than piles in case of loose sand as compared to than in dense sand. As the first excavation progressed the load taken by the raft kept decreasing till excavation reached h/H_e=0.63 in all the cases. Among the four cases simulated, the largest and the smallest amount of reduction of the load taken by the raft resulted from the excavation in the cases of D_r=30% and D_r=90%, respectively. To compensate for the decrease in the load carried out by the raft, the load was transferred to the pile head. However, as excavation proceeds beyond h/H_e=0.63, the load taken by the raft kept increasing till the completion of the excavation in all four cases. This implies that the load is re-transferred to the raft. This is because the deeper excavation led to a substantial settlement in the raft but less ground surface settlement. The load carried by the raft reduced to 5% at the excavation stage h/H_e=0.75 and after that increased to 3% on completion of the excavation.

During the second excavation, similar characteristics of the load transfer between the raft and piles but with different magnitudes were computed to those observed during the first excavation in the sand of with different relative densities. The load taken by the raft decreases during the second excavation (h/H_e=0.75) in all four cases. The load resisted by the raft decreased by 15% and 33% of the initial part of the working load resisted by the raft in cases of D_r=30% and D_r=90%, respectively. As excavation progressed beyond h/H_e=0.75, the load by the raft increased. On completion of the excavation, the load borne by the raft was 26% and 14% of the working load in cases of D_r=30% and D_r=90%, respectively.

3.7 Load redistributions among piles in the piled raft due to excavation

The piled raft supports the load by mobilizing stresses in the ground (Soomro *et al*. 2022a). Since the process of the excavation essentially induced stress release in the ground, load redistribution also occurred among piles in the piled raft.

Fig. 11(a) shows the changes in head load (Δp) of piles P1, P2, P3, and P4 during excavation in loose sand with D_r=30%. The change in the pile head load (Δp) is normalised by the load taken by each pile (p_i) before the excavation. Since twin excavations were carried out on either side of the piled raft (see inset in the figure), the changes in the head loads of the pile closest to the first excavation (piles P1 and P3) and the changes in the head loads of the pile closest to the second excavation (piles P2 and P4) are same during excavation. It can be seen from the figure that the head loads of all four piles increase during the first two excavation stages (h/H_e=0.25). This is because the load resisted by the raft decreases (see Fig. 10) resulting in load transfer to all four piles. However, as the excavation further proceeds, the load at the heads of piles P1 and P3 decreased and the head loads of piles P2 and P4 kept

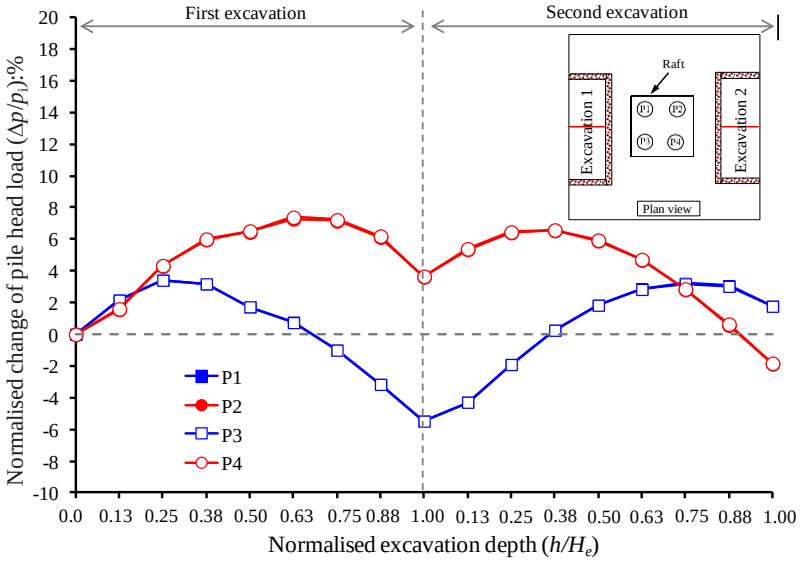

(a)

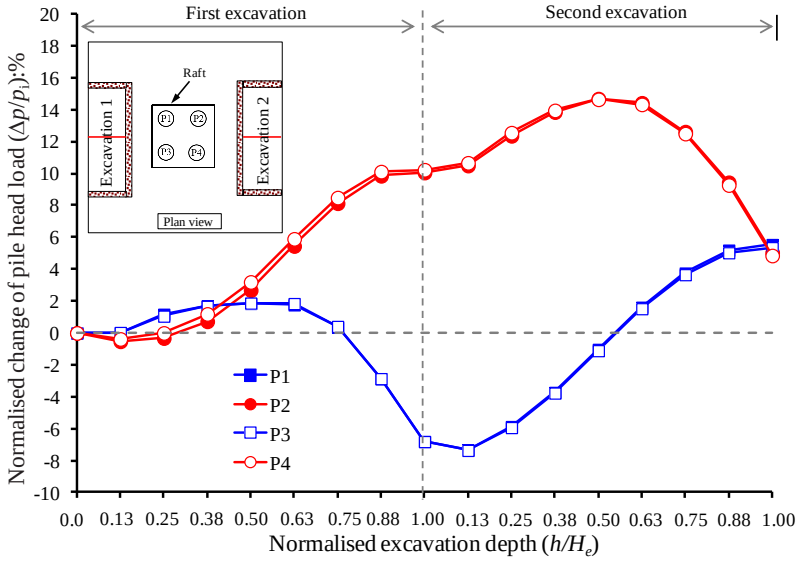

(b)

Fig. 11 Load-redistributions among piles in the piled raft (a) D_r=30%, (b) D_r=90%

increasing. This is because excavation-induced stress release and soil movement towards excavation led to a reduction of shaft resistance along the pile. To support the constant working load acting on the raft, the head load of pile P2, as well as that of pile P4 and the load taken by the raft, increased as a result of load redistribution from piles P1 and P3. During the last two stages of the first excavation (h/H_e=0.88 and 1.00), the head load of all four piles decreased because of the load shared by the raft due to piled settlement. Owing to load redistribution among piles during excavation, the rear piles (i.e., P2 and P4) experienced the most significant increase of 7% in head load. During the subsequent excavation which is closets to piles P2 and P4, the head load of piles P2 and P4 decreased till the end of the second excavation. On another hand, the head loads of piles P1 and P3 (which are farthest from the second excavation) increased during the second excavation as a result of load redistribution from piles P2 and P4. This observation can be attributed to the reduction in shaft resistance of piles P2 and P4 due to excavation-induced stress release. On completion of twin excavations (which are carried out on either side of the piled raft), the head load of all four piles returned to its values prior to excavation.

Compared to load re-distribution among piles during twin excavations in the sand with D_r=30%, a distinct mechanism of the load re-distribution was computed during twin excavation in sand D_r=90% (as illustrated in Fig. 11(b)). Owing to larger tilting of the piled raft in the case of D_r=90%, the head loads of piles P2 and P4 increased significantly. On the hand, the head loads of piles P1 and P3 slightly increased during the initial stages of the first excavation but reduced abruptly as soon as excavation proceeds beyond h/H_e=0.63. This is because of the reduction of shaft resistance due to excavation-induced stress release. Some of the reduced axial load taken by shaft resistance along the upper part of the pile was transferred

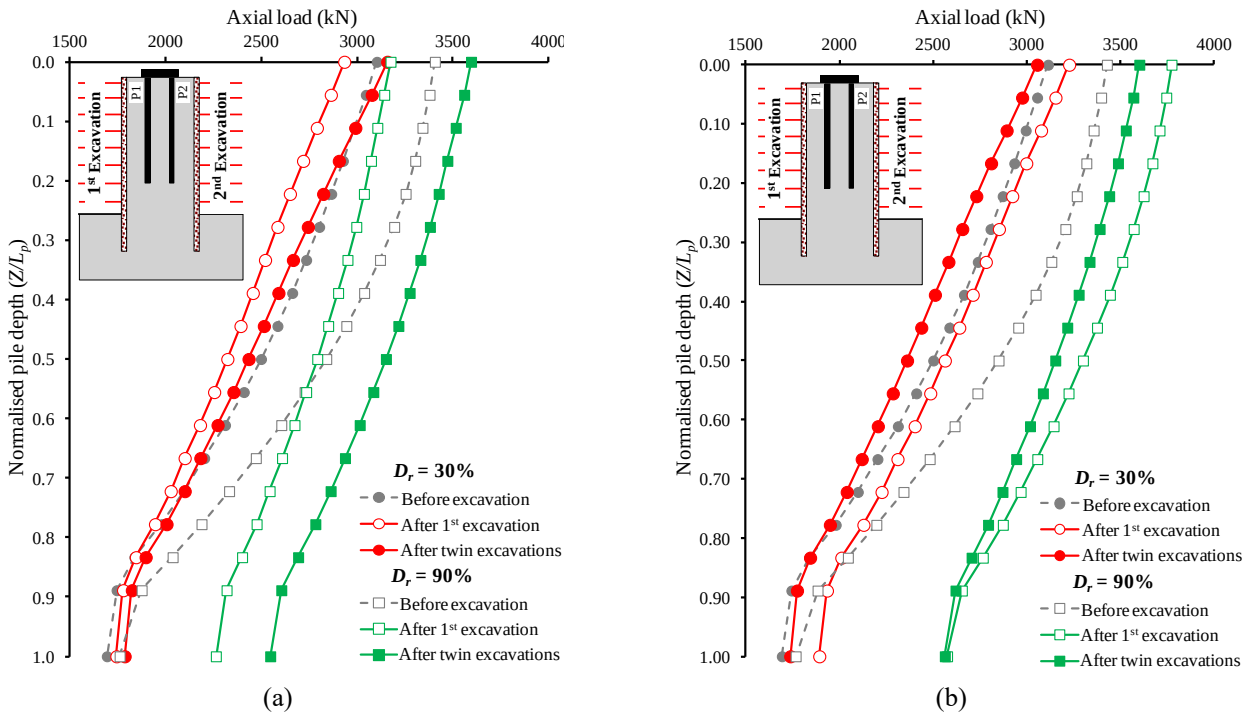

Fig. 12 Axial load distribution after the first excavation and twin excavations along (a) pile P1, (b) pile P2

down to the pile toe (discussed in section 3.8) and partially redistributed to piles P2 and P4 through the rigid raft. The maximum increment of 10% in the head load of piles P2 and P4 was computed on completion of the first excavation. During subsequent exaction closer to piles P2 and P4, the head load of piles P1 and P3 increased substantially throughout the second excavation but head loads of piles P1 and P3 decreased as soon as excavation proceeds beyond h/H_e=0.63. This is because the piled raft tilts towards the second exaction causing the reduction of shaft resistance. Similar to the load re-distribution of pile head loads during the first excavation, the head load of piles P2 and P4 (closest to the second excavation) was redistributed to piles P1 and P3 through the rigid raft. Unlike the load re-distribution among piles due to excavation in loose sand (D_r=30%), the head load of all four piles remained 5% higher than its values prior to excavation.

3.8 Changes in axial load distribution along piles

As discussed in previous sections, the load taken by the raft and head loads of the piles altered substantially during twin excavations. It implies that changes in axial load distribution along 4 piles can be induced due to excavation-induced stress release. Since the arrangement of the 4 piles in the piled raft is in a square pattern (i.e. (2×2) piles), the piles P1 and P2 (see the inset in Fig. 12) are selected for discussion in this section. Figs. 12(a) and (b) compare the axial load distribution along the length of pile P1 and pile P2 on completion of the first and second excavations in loose (D_r=30%) and dense (D_r=90%) sand, respectively. Axial load distribution before excavation (after applying working load) is also included in each figure as a reference line.

As discussed in the previous section, prior to twin excavations, the raft contributes to carry 27% and 17% of the working load (i.e., 16.13 MN) in cases of D_r=30% and D_r=90%, respectively. The remainder of the load (12.4 MN in case of D_r=30% and 13.7 MN in case of D_r=90% was transferred to the four piles. Each of the four piles shared the remainder load equally. The load transferred to each pile head (i.e., 3100 kN) was supported by 45% of mobilizing shaft resistance and 55% of end-bearing of piles in the case of D_r=30%, while in the case of D_r=90%, 48% and 52% of shaft resistance and end-bearing were mobilised, respectively. It can be observed that the axial load decreases along the portion of pile P1 (i.e., $0 \le Z/L_p \le 0.80$) on completion of the first excavation in loose sand (D_r=30%). The reduction in axial load resulted from the reduced shaft resistance (discussed in section 3.9), which was in turn caused by stress release due to the first excavation (see Fig. 7).

This reduction of the load taken by the upper part of the pile was taken by the raft (see Fig. 10) and partially transferred pile P2 through the raft. This led to an increase in the axial load along the entire length of pile P2. To maintain vertical equilibrium, the piled raft has to settle (see Fig. 3) to mobilise more shaft resistance along the upper part of the pile P1 as well as pile P2 (Z/L_p>0.30). In addition, the load was transferred down to the pile toe, leading to a 12% increase in mobilised end-bearing resistance of pile 2. Due to the second excavation near the pile P2, an opposite load transfer mechanism is observed. In other words, the pile closet to the second excavation (i.e., pile P2) experiences a reduction of axial load along the portion of pile P2 (i.e., $0 \le Z/L_p \le 0.80$). The reduction is partially transferred to its neighbouring piles (such as pile P1, see Fig. 11(a)) and some load was taken by the raft (see

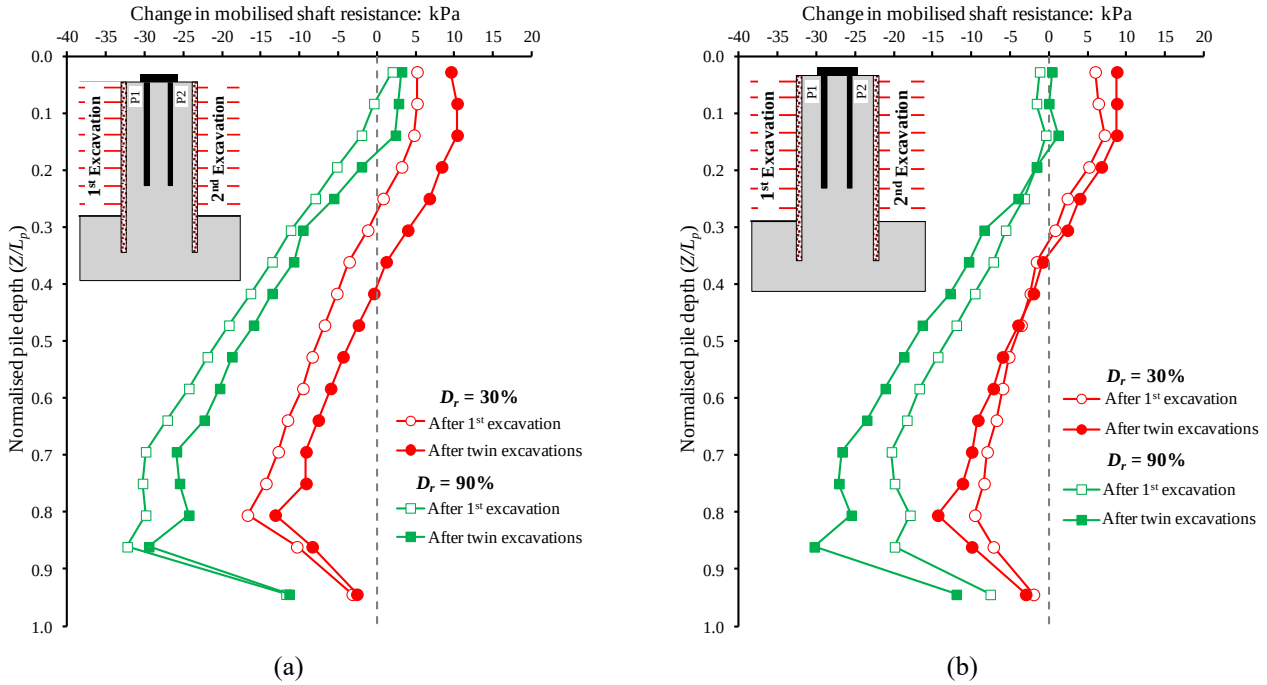

Fig. 13 Changes in mobilised shaft resistance to twin excavations (a) pile P1, (b) pile P2

Fig. 10). This load transfer results in an increase of axial force along the entire length of pile P1. After the twin excavations in the case of D_r=30%, mobilised toe resistance in pile P1 by 5%. The changes in axial load distribution along the length of piled raft suggest that the upward load transfer mechanism occurred due to twin excavation in loose sand.

Owing to twin excavations in dense sand (D_r=90%), a distinct load transfer mechanism is identified. The first excavation caused the reduction of the axial load at mid-depth of pile P1. The major part of the reduced load transfer to the toe of the pile increases the end-bearing of the pile by 30%. The remaining part of the load transferred to the pile P2 which led to increases axial load along the entire length of pile P2. This load transfer mobilise the end-bearing of the pile P2 by 46%. This observation can be attributed to the stiffness of the sand. Because of the higher stiffness of dense sand, the settlement of the piled is smaller compared to the case of loose sand (see Fig. 3). Therefore, the load transfer downward increases the end-bearing of the piles in the case of D_r=90%. Owing to the lower stiffness of loose sand, the piled raft has to settle substantially to mobilise shaft resistance along the pile length and raft resistance as well (see Fig. 10). Due to subsequent excavation near the pile P2 in the case of D_r=90%, an opposite load transfer mechanism is observed. In other words, the pile closet to the second excavation (i.e., pile P2) experiences a reduction of axial load along the entire length of pile P2. The reduction is partially transferred to its neighbouring piles (such as pile P1, see Fig. 11(a)) and some load was taken by the raft (see Fig. 10). This load transfer results in an increase of axial force along the entire length of pile P1 significantly. After the twin excavations in the case of D_r=90%, mobilised toe resistance in pile P1 by 45%. The changes in axial load distribution along the length of piled raft suggest that the downward load transfer mechanism occurred due to twin excavation in dense sand.

3.9 Changes in mobilised shaft resistance along piles

To substantiate the discussion from the previous section, the changes in mobilised shaft resistance along piles P1 and P2 due to twin excavations in loose (D_r=30%) and dense (D_r=90%) sand are depicted in Figs. 13(a) and (b), respectively. The computed average mobilised unit shaft resistance *f(Z)* at various depths was calculated based on the following equation

$$f(Z) = \frac{\Delta Q_{(Z)}}{s.\Delta Z} \quad (4)$$

where ΔQ is the difference between the computed axial loads at two consecutive depths, ΔZ is the vertical distance between the two consecutive depths, and *s* is the perimeter of the pile.

It can be observed that the mobilised shaft resistance decreased along the lower portion of the pile P1 (Z/L_p>0.25) on completion of the first excavation in both cases of D_r=30% and D_r=90%. Compared to the reduction of the shaft resistance in the case of D_r=30% (maximum reduction of 16.8 kPa at Z/L_p=0.8), a higher reduction was computed in the case of D_r=90% (maximum reduction of 32.3 kPa at Z/L_p=0.85).

This is because the lower portion of the pile shaft was subjected to a higher reduction of normal stresses in the case of D_r=90% that in the case of D_r=30% due to the first excavation (see Fig. 7).

To maintain the equilibrium of the piled raft, the load was transferred upward to mobilise shaft resistance, to the raft (see Fig. 10), and pile P2 (see Fig. 11(a)) in the case of D_r=30%. In contrast, to load transfer in case of D_r=30%,

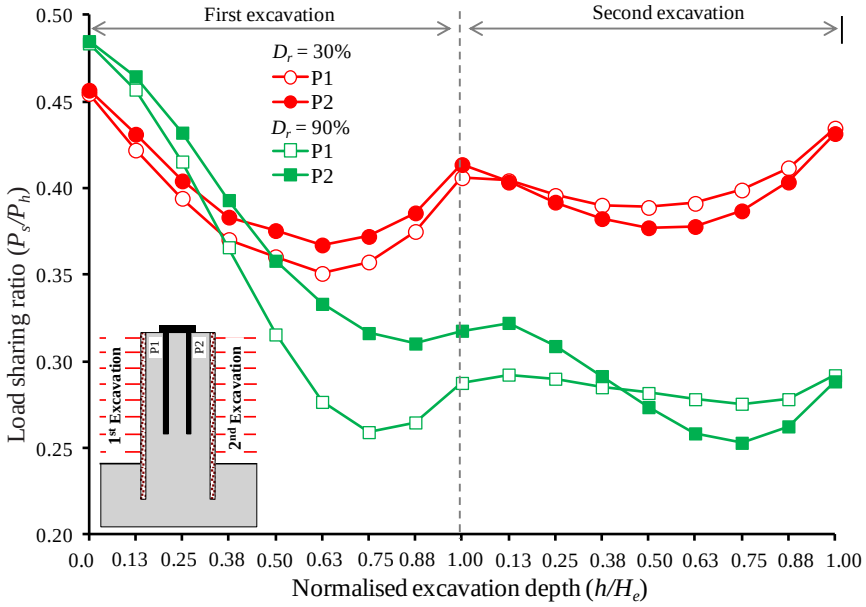

Fig. 14 Load sharing between the shaft and the toe of piles P1 & P2 during twin excavations

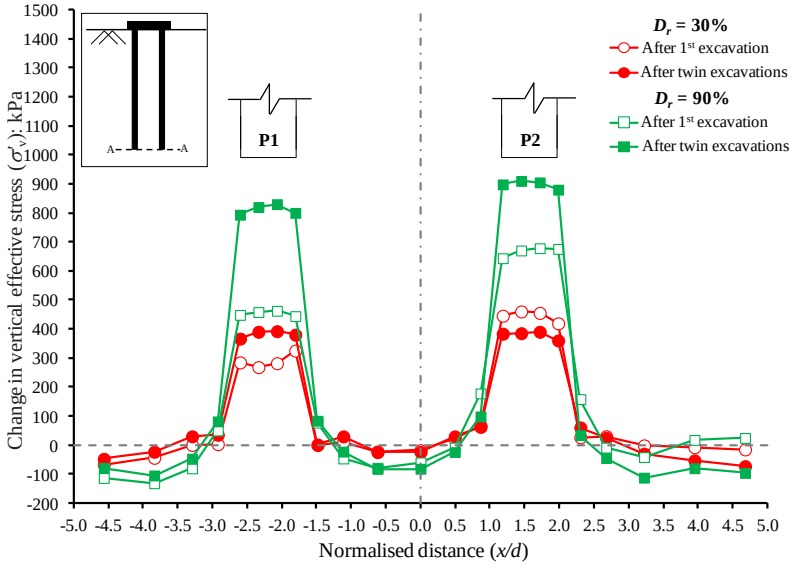

Fig. 15 Change in vertical effective stress below the piled raft due to twin excavations

some of the load was transferred downward to mobilise end-bearing resistance (see Fig. 12), raft, and pile P2 through rigid raft in case of D_r=90%. This is attributed to the smaller stiffness of loose sand than dense sand which resulted in a larger settlement in the piled raft due to the first excavation. The subsequent excavation on the other side of the piled raft caused similar changes in mobilised shaft resistance along the length of both piles P1 and P2 in both cases qualitatively.

3.10 Load sharing between the pile shaft and the pile toe

To understand the load transfer mechanism (i.e., upward and downward) in the piled raft due to twin excavations in loose and dense sand, the load taken by the pile shaft (P_s) is normalised by the total load carried by the pile head (P_h). A load sharing ratio (P_s/P_h ratio) equal to 1 means the head load is fully transferred to the pile shaft (i.e., friction pile) while a P_s/P_h ratio equal to 0 represents the head load is entirely resisted by the pile toe (i.e., end bearing pile). Fig. 14 shows the change of the load sharing ratio in pile P1 and pile P2 with twin excavation stages in cases D_r=30% and D_r=90%. It can be seen that prior to excavation (after application of working load) about 43% and 49% of the load acting on both piles was carried by the pile shaft in cases of D_r=30% and D_r=90%., respectively. This is because of larger normal stress on the pile shafts in the case of D_r=90%. As compared to the shaft resistance due to the first excavation in the case of D_r=30%, a significant reduction in the shaft resistance of both piles P1 and P2 was observed. This is because the lower portion of the pile shaft was subjected to a higher reduction of normal stresses in the case of D_r=90% that in the case of D_r=30% due to the first

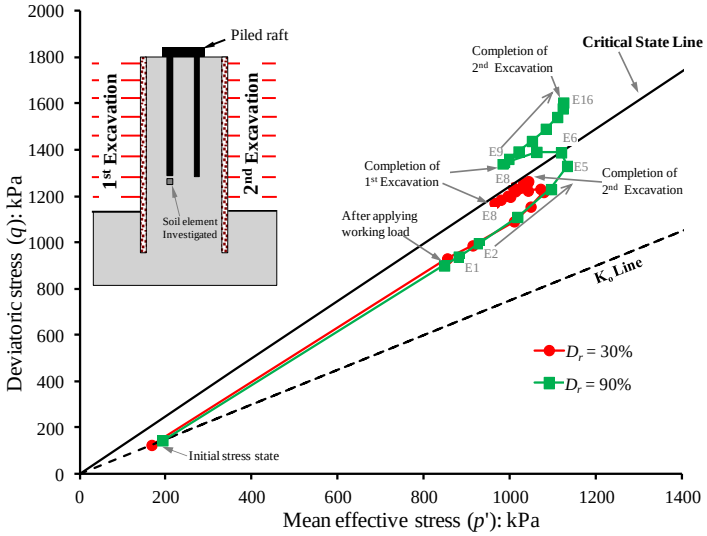

Fig. 16 Stress path evolution a typical soil element below the toe of the pile during twin excavations

excavation (see Fig. 7). This suggests there was a downward load transfer from pile shaft to the pile toe in case of D_r=90% but upward load transfer from pile shaft to the raft was computed in case of D_r=30%. A similar load transfer mechanism was observed during the subsequent excavation in both cases. At the end of the twin excavation, about 43% and 29% of the total load transferred to the piles P1 and P2 were carried by the pile shaft in cases of D_r=30% and D_r=90%., respectively.

3.11 Stress transfer mechanism in the ground underneath the piled raft during twin excavations

To substantiate the discussion of the load transfer mechanism in the piled raft due to twin excavations in loose and dense sand identified in previous sections, changes in stresses in the ground underneath the piled raft are explored in this section.

3.11.1 Mobilised shear stiffness of soil element underneath the pile toe

Fig. 15 shows the computed change in vertical effective stress (σ'_v) in the soil immediately below the toe of the piled raft (along section A-A) due to twin excavations in the case of D_r=30% and D_r=90%. The figure depicts the vertical stress increase after the excavation below P1 and P2, inferring a load transfer from the shaft to the toe of the piles due to the mobilization of the end bearing resistance as compensation for the reduction in positive shaft resistance. The increase in vertical stress below the piled raft due to the first excavations in the case of D_r=90% is greater than that in the case of D_r=30%. This clearly suggests that the load transferred to the pile toe to further mobilise the end-bearing of the pile toe (see Fig. 12) in the case of D_r=90%. As with the first excavation, the second excavation (on the other side of the piled raft) in both cases also led to an increase in vertical stress underneath both piles P1 and P2. A difference in the settlement is caused between the front and rear piles by a non-uniform change in stress which resulted in pile raft tilting (see Fig. 4).

3.11.3 Computed stress path soil element underneath the pile toe

Fig. 16 computed stress paths of a soil element located right below pile P1 during twin excavations in loose (D_r=30%) and dense (D_r=90%) sand. The K_0 (at-rest earth pressure coefficient) line and critical state line are also shown in the figure for reference.

It can be seen that the initial stress states of the selected soil element in both cases are at K_0 stress condition as expected. After applying a working load to the piled raft in both cases, the mean effective stress (p') and deviatoric stress (q) of the selected soil element increased in both cases. As a result, the stress path moved towards the critical state line. As the first excavation (from E1 to E8) proceeds in the case of dense sand, both p'and q increased due to downward stress transfer from the pile shaft to the pile toe (see Fig. 12). As a result, the stress path moved towards the critical state line and reached failure once the excavation reaches E6 (h/H_e=0.75). The second excavation (from E9 to E16) resulted in further increases in both p'and q at a lower rate than that during the first excavation. This is because the downward stress transfer during the second excavation was more substantial than that during the first excavation (see Fig. 14). As a result, the stress path moved beyond the critical state line. The stress paths in the case of D_r=30% show a similar trend to that in the case of D_r=90% but with a smaller change in magnitude. This suggests that the upward stress transfer (from the pile toe to the pile shaft, see Fig. 14) during twin excavations.

4. Conclusions

In this study, three-dimensional numerical analysis was carried out to investigate the influence of sand density on an existing (2×2) piled raft (with working load on top of the raft) due to twin excavations. A wide range of relative density (D_r) from loosest (30%), loose to medium (50% and 70%) and densest (90%) were selected to investigate the effects on settlement and load transfer mechanism of piled

raft during twin excavations. An advanced hypoplastic sand model (which can capture small-strain stiffness and stress-state dependent dilatancy of sand) was adopted. It should be noted that the computed results reported in this paper should be treated with caution since they may be specific to the particular soil type and isolated wall type adopted.

(a) Twin excavations in loose sand (D_r=30%) caused the most significant settlement. This is because of the higher stiffness of denser sand (D_r=90%) than that of loose sand. Similar characteristics and magnitudes of piled raft settlement during the second excavation were computed to those observed during the first excavation in the sand with different relative densities.

(b) Unlike piled raft settlement (whose maximum value occurs at the end of twin excavation) in each case, the most significant transverse tilting of the piled raft is induced after the completion of the first excavation. A much larger maximum differential settlement (tilting) was computed in dense sand than in loose sand (0.18%) which is within the allowable limit (0.2%) suggested by Eurocode 7 (CEN, 2001). This is because the twin excavation in dense sand led to the largest non-uniform change (212 kPa) in vertical effective stress underneath all piles in the piled raft.

(c) As far as load transfer mechanism along the piles is concerned, an upward load transfer to mobilise shaft resistance is observed in loose sand. The load transferred to the raft and partially redistributed to piles P2 and P4 through the rigid raft. The head load of pile P2, as well as that of pile P4 and the load taken by the raft, increased as a result of load redistribution from piles P1 and P3.

(d) On the contrary, a downward load transfer is observed in dense sand. A higher shaft resistance was computed in the case of *Dr*=90% (maximum reduction of 32.3 kPa at Z/L_p=0.85). To maintain the equilibrium of the piled raft, some of the load was transferred downward to mobilise end-bearing resistance and pile P2 through rigid raft in case of D_r=90%. This is attributed to the smaller stiffness of loose sand than dense sand which resulted in a larger settlement in the piled raft due to twin excavation.

Acknowledgments

The authors would like to acknowledge the financial support provided by Mehran University of Engineering & Technology, Jamshoro, Sindh and Pakistan.

References

Fang, J., Kong, G. and Yang, Q. (2022), "Group performance of energy piles under cyclic and variable thermal loading", *J. Geotech. Geoenviron. Eng.*, **148**(8), 04022060. https://doi.org/10.1061/(ASCE)GT.1943-5606.0002840.

Finno, R.J., Lawrence, S.A., Allawh, N.F. and Harahap, I.S. (1991), "Analysis of performance of pile groups adjacent to deep excavation", *J. Geotech. Eng.*, **117**(6), 934-955. https://doi.org/10.1061/(ASCE)0733-9410(1991)117:6(934).

Goh, A.T.C., Wong, K.S., Teh, C.I. and Wen, D. (2003), "Pile response adjacent to braced excavation", *J. Geotech. Geoenviron. Eng.*, **129**(4), 383-386. https://doi.org/10.1061/(ASCE)1090-0241(2003)129:4(383).

Gudehus, G. (1996), "A comprehensive constitutive equation for granular materials", *Soil. Found.*, ***36***(1), 1-12. https://doi.org/10.3208/sandf.36.1.

Herle, I. and Gudehus, G. (1999), "Determination of parameters of a hypoplastic constitutive model from properties of grain assemblies", *Mech. Cohes.-Frict. Mater.: J. Exper., Model. Comput. Mater. Struct.*, **4**(5), 461-486. https://doi.org/10.1002/(sici)1099-1484(199909)4:5%3C461::aid-cfm71%3E3.0.co,2-p.

Hibbitt, Karlsson, Sorensen (2010), Abaqus User's Manual, Version 6.10.2, Hibbitt, Karlsson & Sorensen Inc., Providence, RI, USA.

Ishihara, K. (1993), "Liquefaction and flow failure during earthquakes", *Géotechnique*, **43**(3), 351-415. https://doi.org/10.1680/geot.1993.43.3.351.

Jáky, J. (1944), "The coefficient of earth pressure at rest", *J. Soc. Hungarian Arch. Eng*., 355-358. (in Hungarian)

Karira, H., Kumar, A., Ali, T.H., Mangnejo, D.A. and Mangi, N. (2022), "A parametric study of settlement and load transfer mechanism of piled raft due to adjacent excavation using 3D finite element analysis", *Geomech. Eng.*, **30**(2), 169-185. https://doi.org/10.12989/gae.2022.30.2.169.

Korff, M., Mair, R.J. and Van Tol, F.A. (2016), "Pile-soil interaction and settlement effects induced by deep excavations", *J. Geotech. Geoenviron. Eng*., **138**(7), 04016034. https://doi.org/10.1061/(ASCE)GT.1943-5606.0001434.

Lee, S.W. (2019), "Experimental study on effect of underground excavation distance on the behavior of retaining wall", *Geomech. Eng.*, **17**(5), 413-420. https://doi.org/10.12989/gae.2019.17.5.413.

Liyanapathirana, D.S. and Nishanthan, R. (2016), "Influence of deep excavation induced ground movements on adjacent piles", *Tunnel. Undergr. Space Technol.*, **52**, 168-181. https://doi.org/10.1016/j.tust.2015.11.019.

Maeda, K. and Miura, K. (1999), "Relative density dependency of mechanical properties of sands", *Soil. Found.*, **39**(1), 69-79. https://doi.org/10.3208/sandf.39.69.

Ng, C.W., Shakeel, M., Wei, J. and Lin, S. (2021), "Performance of existing piled raft and pile group due to adjacent multipropped excavation: 3D centrifuge and numerical modeling", *J. Geotech. Geoenviron. Eng.*, **147**(4), 04021012.. https://doi.org/10.1061/(ASCE)GT.1943-5606.0002501.

Ng, C.W., Wei, J., Poulos, H. and Liu, H. (2017), "Effects of multipropped excavation on an adjacent floating pile", *J. Geotech. Geoenviron. Eng.*, **143**(7), 04017021. https://doi.org/10.1061/(ASCE)GT.1943-5606.0001696.

Niemunis, A. and Herle, I. (1997), "Hypoplastic model for cohesionless soils with elastic strain range", *Mech. Cohes.-Frict. Mater.: J. Exper., Model. Comput. Mater. Struct.*, **2**(4), 279-299. https://doi.org/10.1002/(SICI)1099-1484(199710)2:4<279::AID-CFM29>3.0.CO,2-8.

Poulos, H.G. (2001), "Piled raft foundations: Design and applications. *Géotechnique*, **51**(2), 95-113. https://doi.org/10.1680/geot.2001.51.2.95.

Shi, J., Chen, Y., Lu, H., Ma, S. and Ng, C.W.W. (2022a), "Centrifuge modeling of the influence of joint stiffness on pipeline response to underneath tunnel excavation", *Can. Geotech. J.*, **59**(9), 1. https://doi.org/10.1139/cgj-2020-0360.

Shi, J., Wei, J., Ng, C. W. and Lu, H. (2019), "Stress transfer mechanisms and settlement of a floating pile due to adjacent multi-propped deep excavation in dry sand", *Comput. Geotech.*, **116**, 103216. https://doi.org/10.1016/j.compgeo.2019.103216.

Shi, J., Wei, J., Ng, C.W., Lu, H., Ma, S., Shi, C. and Li, P.

(2022b), "Effects of construction sequence of double basement excavations on an existing floating pile", *Tunnel. Undergr. Space Technol.*, **119**, 104230. https://doi.org/10.1016/j.tust.2021.104230.

Soomro, M.A., Kumar, M., Mangi, N., Mangnejo, D.A. and Cui, Z.D. (2022b), "Parametric study of twin tunneling effects on piled foundations in stiff clay: 3D finite-element approach", *Int. J. Geomech.*, **22**(6), 04022079. https://doi.org/10.1061/(ASCE)GM.1943-5622.0002386.

Soomro, M.A., Liu, K., Mangnejo, D.A. and Mangi, N. (2022c), "Effects of twin excavations with different construction sequence on a brick masonry wall: 3D finite element approach", *Struct.*, **41**, 866-886. https://doi.org/10.1016/j.istruc.2022.05.060.

Soomro, M.A., Mangi, N., Memon, A.H. and Mangnejo, D.A. (2022a), "Responses of high-rise building resting on piled raft to adjacent tunnel at different depths relative to piles", *Geomech. Eng.*, **29**(1), 25-40. https://doi.org/10.12989/gae.2022.29.1.025.

Soomro, M.A., Mangnejo, D.A., Saand, A. and Hong, Y. (2021a), "Responses of a masonry façade to multi-propped deep excavation-induced ground deformations: 3D numerical parametric study", *Eur. J. Environ. Civil Eng.*, 1-29. https://doi.org/10.1080/19648189.2021.1926336.

Soomro, M.A., Mangnejo, D.A., Saand, A. and Mangi, N. (2021c), "3D numerical analysis of a masonry façade subjected to excavation-induced ground deformation", *Int. J. Geotech. Eng.*, **16**(7), 865-877. https://doi.org/10.1080/19386362.2021.1937853.

Soomro, M.A., Mangnejo, D.A., Saand, A., Mangi, N. and Auchar Zardari, M. (2021b), "Influence of stress relief due to deep excavation on a brick masonry wall: 3D numerical predictions", *Eur. J. Environ. Civil Eng.*, 1-24. https://doi.org/10.1080/19648189.2021.2004450.

Soomro, M.A., Saand, A., Mangi, N., Mangnejo, D.A., Karira, H. and Liu, K. (2021d), "Numerical modelling of effects of different multipropped excavation depths on adjacent single piles: Comparison between floating and end-bearing pile responses", *Eur. J. Environ. Civil Eng.*, **25**(14), 2592-2622. https://doi.org/10.1080/19648189.2019.1638312.

GC